DEVELOPMENT OF A C-BAND PULSE COMPRESSION WEATHER RADAR

Katsuhiro NAKAGAWA[1], Hiroshi HANADO[2], Kouichi FUKUTAN[3], and Toshio IGUCHI[1]

[1]National Institute of Information and Communications Technology, Japan
[2]JAXA, Japan
[3]NEC Corporation, Japan

1. INTRODUCTION

In Japan, the frequency assignment for weather radar is between 5250 and 5350 MHz in the C-band. Mutual interference among radars has become a problem with the increase in the number of weather radars. It is thus necessary to develop technology to decrease the interference. The National Institute of Information and Communications Technology (NICT) has developed equipment for weather radar that modulates the transmitting signal and demodulates the received signal (i.e., a pulse compression function). This equipment has been added to the existing COBRA system, forming a new system referred to as COBRA+.

2. COBRA+ SYSTEM

The original COBRA system uses two klystron transmitter units for polarization observations (Nakagawa et al. 2003), whereas the COBRA+ system uses two traveling-wave tube amplifier (TWTA) transmitter units, because a TWTA can transmit a signal modulated by both frequency and amplitude. The main specifications of COBRA+ are listed in Table 1. The peak power of the TWTA is 10 kW. The signal/data processing subsystem of COBRA was also modified to demodulate the received signal according to the modulated transmitted signal. The two TWTA transmitters units are also used to observe polarizations. The transmission polarization for each pulse is selected from among six possible polarizations: horizontal polarization, vertical polarization, ±45-degree-tilt linear polarizations, and right- and left-handed circular polarizations. A compressed pulse (long pulse) and uncompressed pulse (short pulse) can be transmitted at each pulse and by every beam. The observation mode can be switched mechanically between COBRA (klystron transmitters) and COBRA+ (TWTA transmitters) within a few seconds.

The polarization parameters shown in Fig. 1 are calculated in the COBRA/COBRA+ system. They include the differential reflectivity between the horizontal and vertical polarizations, ZDR (=ZHH/ZVV); the linear depolarization ratio, LDR (=ZHV/ZHH); the cross-correlation coefficient, ρHV(0); and the differential propagation phase between the horizontal and vertical polarizations, ΦDP (and its derivative in the range direction, KDP) (M. Sachidananda et al. 1986; R. J. Doviak et al. 1993; V. N. Bringi et al. 2001).

TABLE 1 Specifications of the COBRA+/COBRA system

|	
Peak power	> 250 kW (Dual Klystron, COBRA) > 10 kW (Dual TWTA, COBRA+)
Pulse width	0.5 μs, 1.0 μs, 2.0 μs (COBRA) 0.5 – 100 μs (COBRA+)
PRF	250 Hz - 3000 Hz, PRT 1μ step (staggered PRF)
Antenna size	4.5m diameter parabolic
Beam width	0.91 deg
Radome size	8m diameter
Cross pol. ratio	> 36 dB (Integrated value in a beam)
Antenna gain	45 dBi (including radome)
Sidelobe	< -27 dB (one way)
Ant. scan speed	0.5-10 rpm(PPI), 0.1-3.6 rpm(RHI), 0.1 rpm step
Polarization	H, V, +45, -45, LC, RC (pulse by pulse)
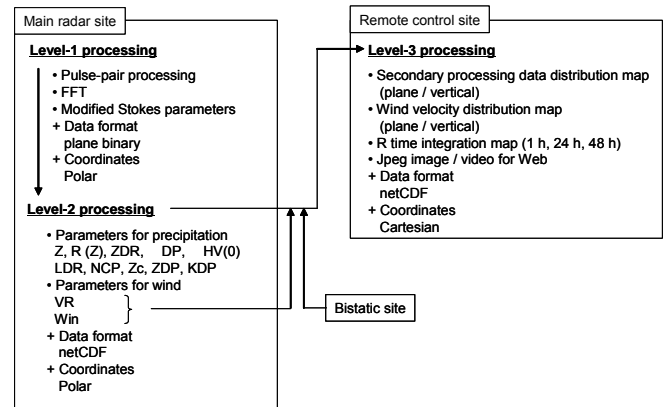
Fig. 1 Block diagram of the signal and data flow in the COBRA/COBRA+ system

3. PULSE-COMPRESSION TECHNIQUES

Pulse-compression schemes for improving radar range resolution were first theoretically described in Woodward's (1953) fundamental paper. Chadwick and Cooper (1972) and Keeler and Frush (1983) have described the principle of using distributed targets for pulse-compression Doppler measurements with microwave weather radars.

Corresponding author address:
Katsuhiro NAKAGAWA, Okinawa Subtropical Environment Remote-sensing Center, National Institute of Information and Communications Technology, 4484 Aza-Onna, Onna, Kunigami, Okinawa 904-0411, Japan; e-mail: nakagawa@nict.go.jp.

The disadvantages of pulse compression are range sidelobes   and blind range. When looking at the output of a pulse-compression radar, the sidelobes on either side of the central pulse, called range sidelobes, are reasonably large. Range sidelobes are especially troublesome in high reflectivity gradients. Because atmospheric targets are distributed in space, integrated sidelobes contribute to distortion. They are analogous to integrated antenna sidelobes that contribute interference from distributed targets at the same distance (Keeler and Frush, 1983). The solution to the range sidelobe problem is to apply linear frequency modulation (chirp) and demodulation using a window function, namely a Blackman-Harris 4–term window. This technique has been investigated for downward-looking radars on air or space platforms, and it is well suited to Doppler observation.

We simulated the suppression effects for range sidelobes with three modulation methods: (a) linear chirp, (b) pre-distortion chirp, and (c) raised cosine. In the simulation, the pulse widths for a long pulse and a compressed pulse were 64 and 0.5 μs, respectively, giving a compression ratio of 128. Figure 2 shows the transmitted frequency for pre-distortion chirp, where δf_p and δt are defined as follows:

$$\begin{cases} f_p = 0.1 \times (K_f - 1) \times 10^6 + 2.0 \times 10^6 \\ \quad = 2.2MHz (K_f = 3) \\ \delta t = K_t \times t_s \\ \quad = 0.625 \mu s (t_s = 0.125 \mu s, K_t = 5) \end{cases} .$$

Fig. 3 shows the waveform for the raised cosine method, where $wa1$, $wa2$, and $wa3$ are defined as follows:

$$wa(t) = \begin{cases} wa1 = 0.5\left\{1 - \cos\left(\dfrac{\pi t}{(T/3)}\right)\right\}, (0 \le t \le T/3) \\ wa2 = 1, (T/3 \le t \le 2T/3) \\ wa3 = 0.5\left\{1 - \cos\left(\dfrac{\pi(t+T/3)}{(T/3)}\right)\right\}, (2T/3 \le t \le T) \end{cases} .$$

Fig. 4 shows the compressed pulse waveforms for each of the modulation methods. The range sidelobes for pre-distortion chirp are below –50 dB, making this method better than linear chirp. For the raised cosine modulation method, however, the range sidelobes are below –60 dB. Raised cosine is clearly the most effective method for suppressing range sidelobes.   Fig. 5 compares the spurious radiation levels for each pulse compression method. From this figure, it is clear that raised cosine also offers the lowest spurious radiation level.

The blind range problem is caused by the fact that a monostatic pulse radar cannot transmit and receive simultaneously. Therefore, the radar is blind whenever it is transmitting. The blind range of a pulse-compression radar is larger than that of a non-pulse-compression (single-pulse) radar, because

the pulse-compression radar transmits a long-duration, low-power pulse. The dual-cycle observation technique provides a solution to this problem. In this technique, the radar changes between a non-pulse-compression (single-pulse) mode and a long-pulse-transmitting (pulse-compression) mode with every beam (as shown in Fig. 6) or every pulse.
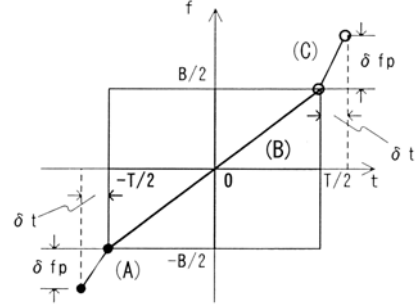
Fig. 2 Transmitted frequency for pre-distortion chirp, with T = 64 μs and B = 2.0 MHz. The values of δf_p and δt are 2.2 MHz and 0.625 μs, respectively. The part indicated by (B) represents linear chirp, while parts (A) and (C) were changed in this method.
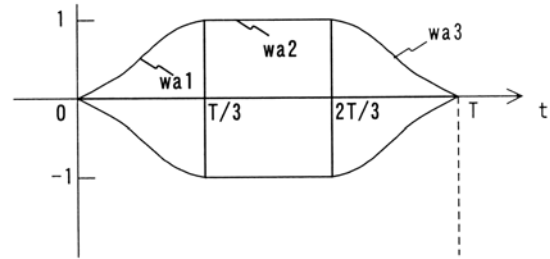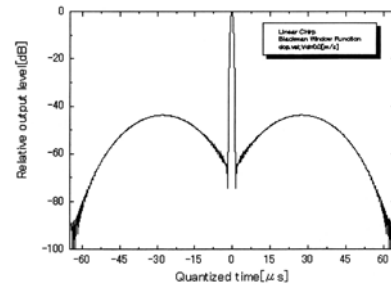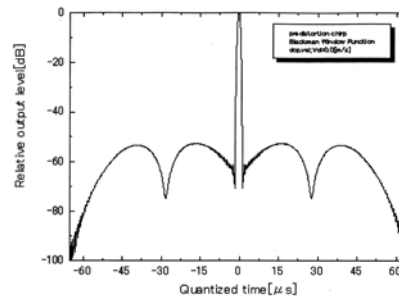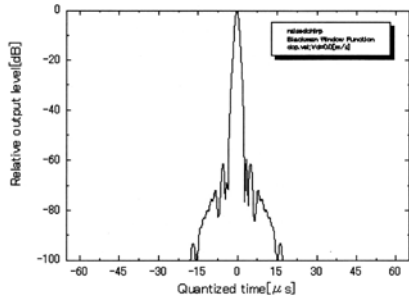
Fig. 3 Waveform for the raised cosine modulation method, with T = 63 μs.

(a) Linear chirp

(b) Pre-distortion chirp

(c) Raised cosine

Fig. 4 Compressed pulse waveforms for each modulation method: (a) linear chirp, (b) pre-distortion chirp, and (c) raised cosine. The horizontal axis indicates the time, and the vertical axis indicates the relative output level.
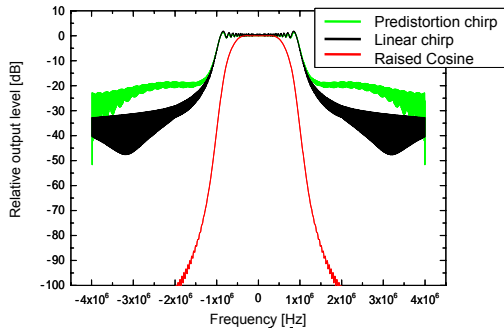

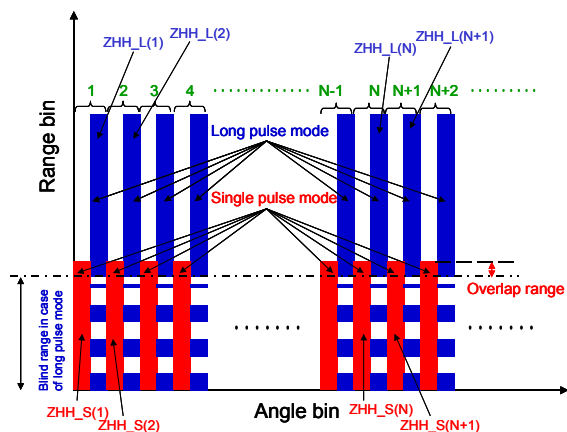Fig. 5 Comparison of the spurious radiation levels for each pulse compression method.


Fig. 6 Conceptual diagram of dual-cycle observation

4. OBSERVATION RESULTS

Typhoon SONGDA approached and passed over the main island of Okinawa, Japan, from Sep. 5 to Sep. 6, 2004. COBRA+ was used to observe the typhoon with the dual-cycle observation technique. Figure 7 shows the horizontal distribution of the radar reflectivity. The pulse widths for long and compressed pulses were

100 and 1.0 μs, respectively, giving a compression ratio of 100. In Fig. 7(a), a blind range area around the radar site, with a diameter of 15 km, can be seen. Figure 7(b) shows the combined distribution obtained using the dual-cycle observation technique. The blind range area was clearly removed very well.
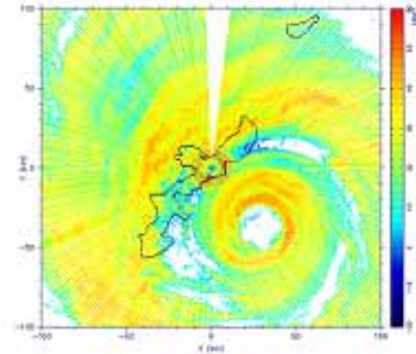
(a) Original distribution
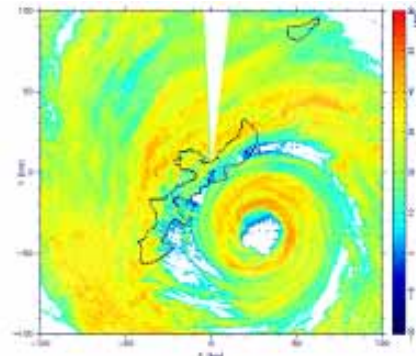
(b) Combined distribution

Fig.7 Horizontal distribution of the radar reflectivity, including (a) the original distribution observed by COBRA+ and (b) the combined distribution obtained using the dual-cycle observation technique. The elevation angle was 0.2°.

Using the overlap range of the long-pulse and single-pulse modes (shown in Fig. 6), we also carried out a quantitative evaluation with COBRA+. Fig. 8 shows a comparison of the radar reflectivities observed with the long-pulse and single-pulse observation modes. The black dots show the single-pulse observation results between ZHH_S(N) and ZHH _s(N+1), the blue dots show the long-pulse results between ZHH_L(N) and ZHH_L(N+1), and the yellow dots represent the comparison between ZHH_S(N) and ZHH_L(N). N is the angle bin number. The correlation coefficient of ZHH_S(N) and ZHH_L(N) is 0.92. The differences between ZHH_S(N) and ZHH_L(N) were strictly caused by the difference in the beams. Therefore, it is clear that the pulse-compression technique works very well for weather radar.
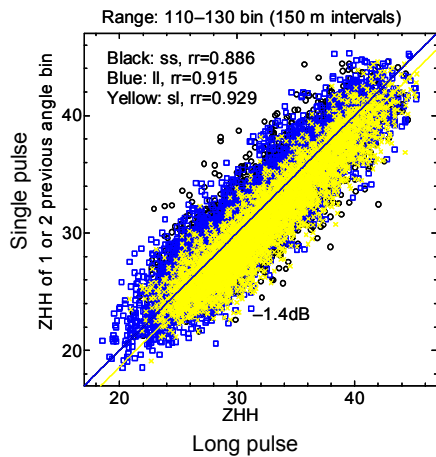
Fig. 8 Comparison of the radar reflectivities observed with the long-pulse and single-pulse observation modes. The black dots: the single-pulse observation results between ZHH_S(N) and ZHH _s(N+1). The blue dots: the long-pulse results between ZHH_L(N) and ZHH_L(N+1). The yellow dots: the comparison between ZHH_S(N) and ZHH_L(N). N is the angle bin number.

5. SUMMARY

In developing a pulse-compression weather radar, the key problems of range sidelobes and blind range must be solved. To obtain a solution to the range sidelobe problem, we simulated the suppression effects, in terms of the range sidelobes and the spurious radiation levels, with three modulation methods: (a) linear chirp, (b) pre-distortion chirp, and (c) raised cosine. From this simulation, we found that the raised cosine pulse-compression method provided good suppression of both the range sidelobes and spurious radiation.

To obtain a solution to the blind range problem, we used the COBRA+ system to observe Typhoon Songda by using the dual-cycle observation technique. From the results of comparing the horizontal distribution of the radar reflectivity between the original distribution and the combined distribution, it was clear that the blind range area was removed very well. We also carried out a quantitative evaluation by using the overlap range of the long-pulse and single-pulse modes. As a result, we clarified that the pulse-compression technique works very well for weather radar.

6. ACKNOWLEGMENT

7. REFERENCES

K. Nakagawa, H. Hanado, S. Satoh, N. Takahashi, T. Iguchi and K. Fukutani, 2003: Development of a new C-band bistatic polarimetric radar and observation of typhoon events.
  Proc. 31st Conf Radar Meteor, AMS, vol. 2, 863-866.

R. J. Doviak and D. S. Zrnic, 1993: Doppler radar and weather observations.
  2nd ed., Chaps. 6 and 8, Academic Press.

M. Sachidananda and D. S. Zrnic, 1986: Differential propagation phase shift and rainfall rate estimation.
  Radio Sci., **21**, 23-247.

V. N. Bringi and V. Chandrasekar, 2001: Polarimetric Doppler Weather Radar -Principiles and applications-.
  Cambridge University Press

P. M. Woodward, 1953: Probability and Information Theory with Applications to Radar.
  Pergamon Press.

R. J. Keeler and C.L. Frush, 1983: Coherent wideband processing of distributed radar targets.
  Dig. Int. Geosci. And Remote Sensing Sympo, pp. 3.1-3.5.

R. B. Chadwick and G. R. Cooper, 1972: Measurement of distributed targets with random signal radar.
  IEEE Trans. Aerosp. Electron. Syst., AES-8, 743-750.